AIP | Journal of Applied Physics

Conductivity enhancement of poly(3,4-ethylenedioxythiophene)-poly(styrenesulfonate) films post-spincasting

Abdiaziz A. Farah, Steven A. Rutledge, Antje Schaarschmidt, Roger Lai, Justin P. Freedman et al.

Citation: J. Appl. Phys. **112**, 113709 (2012); doi: 10.1063/1.4768265
View online: http://dx.doi.org/10.1063/1.4768265
View Table of Contents: http://jap.aip.org/resource/1/JAPIAU/v112/i11
Published by the American Institute of Physics.

Conductivity enhancement of poly(3,4-ethylenedioxythiophene)-poly(styrenesulfonate) films post-spincasting

Abdiaziz A. Farah, Steven A. Rutledge, Antje Schaarschmidt, Roger Lai, Justin P. Freedman, and Amr S. Helmy[a)]
Edward S. Rogers Sr. Department of Electrical and Computer Engineering, University of Toronto, 10 Kings College, Toronto, Ontario, Canada M5S 3G4

(Received 17 September 2012; accepted 1 November 2012; published online 7 December 2012)

Poly(3,4-ethylenedioxythiophene)-poly(styrenesulfonate) (PEDOT:PSS) thin films on indium tin oxide and glass substrates have been fabricated and subjected to a non-adiabatic annealing process. The films showed subtle changes in their structure and optical properties as well as an increase in conductivity due to the effects of rapid thermal annealing. Through a combination of Raman spectroscopy, X-ray photoelectron spectroscopy and atomic force microscopy studies in conjunction with electrical characterization, and four-point probe measurements, material enrichment of conductive PEDOT domains at the polymer-metal interface have been demonstrated, which well explains the surface conductivity improvement of a thin film of PEDOT:PSS after annealing. © *2012 American Institute of Physics*. [http://dx.doi.org/10.1063/1.4768265]

INTRODUCTION

Plastic electronics offers a versatile platform for providing transparent, flexible, large scale circuits. For this to be more commercially viable, the attributes of the existing elements that make up plastic electronics need to be enhanced. Materials' stability is one important example where improvements can be made. Another significant example is the electrical transport properties of the organic semiconducting materials from which plastic electronics are made.[1,2] Several organic semiconducting compounds emerged recently with modified chemical architectures and physical properties that are tailored towards this aim. A great deal of research has been devoted to enhancing organic material transport properties through material processing that enables the optimization of their structural and molecular order.[3,4] Poly(3,4-ethylenedioxythiophene)-poly(styrenesulfonate) (PEDOT:PSS) has emerged to the forefront of these developments in the last decade due to its promising physical, electrical, and chemical properties.[5] The advantage of PEDOT:PSS over its counterparts is that it is highly stable, with controllable morphology and relatively high conductivity. As such, PEDOT:PSS has been utilized to enable highly stable optoelectronic devices including light-emitting diodes, solar cells, thin films transistors, capacitors, smart windows, and sensors.[6] As PEDOT:PSS is being utilized in an increasing number of applications, more research has been directed towards developing techniques to further improve its attributes without compromising its stability and other beneficial properties. Carrier mobility and the associated layer conductivity are of paramount importance for the aforementioned device applications. The relatively lower carrier mobility in organic materials such as PEDOT:PSS in comparison to inorganic crystalline materials poses stringent limitations on the carrier-photon conversion efficiency of organic light emitting devices.[7] Low mobility also impedes high carrier injection and hence is partly responsible for making electrically pumped organic lasers an untenable aim. As such, significant effort has been aimed at enhancing semiconductor polymer carrier mobility through the optimization of their structural and molecular order.[8] One of the techniques that has been previously exploited to improve these properties is thermal annealing in ovens. It has been demonstrated that the crystalline morphology and the orientation of spin cast conjugated polymers films could be modestly improved through oven thermal annealing or melt crystallization approaches.[9] These processes are attractive as they offer a route to control the film properties after casting on the substrate.

The intra-and intermolecular structure inherent to PEDOT:PSS as well as the associated micro-phase behaviour are some of the chief properties that strongly impact the physical characteristics unique to this class of materials. Changes in this specific chemical architecture can lead to significant variations in the physical properties of resultant structural forms. Modifications to the chemical architecture and morphology of spin cast PEDOT:PSS has been recently achieved through the use of non-adiabatic thermal processing; namely rapid thermal annealing approach (RTA).[9] Also, improvement to the crystalline morphology of water soluble CdTe polymer encapsulated quantum dots was achieved using the same annealing technique.[8] RTA is an attractive process, as it offers a route to control and manipulate thin film properties after casting on the substrate beyond what is achievable using conventional oven-based annealing.[10] In this study, we examine the influence of the RTA annealing temperature on the optical and morphological properties of PEDOT:PSS film. The conductivity changes in the annealed films were studied using four point probe and transmission line measurements (TLMs), which were performed to analyze the electrical effects of RTA on the sheet resistivity of the spincast films on glass substrates. In addition, Raman spectroscopy, X-ray photoelectron spectroscopy (XPS), and atomic force microscopy (AFM) were carried out on the

[a)]a.helmy@utoronto.ca.

samples undergoing the same annealing conditions. All these techniques shed light on the extent of which the main chain π-conjugation of PEDOT:PSS and structural phase morphology is directly influenced by the RTA. The spectroscopic properties of PEDOT:PSS were studied for films that are spincast on indium tin oxide (ITO) films on glass. ITO was chosen due to its high conductivity and transparency over the visible spectrum. Also due to its widespread use as a contact layer in various optoelectronic applications including solar cell and organic light emitting diodes.[11]

ELECTRICAL PERFORMANCE MODIFICATION WITH ANNEALING

The influence of the RTA process on PEDOT:PSS films was first investigated using electrical measurements. Insulating glass substrates were first cleaned in a Phantom RIE using oxygen plasma for 5 min to remove any trace organic material. For electrical characterization, PEDOT:PSS was spincast on the glass in a single cast at 2000 RPM for 45 s, and then soft baked at 105 °C for 5 min in ambient air. The resulting PEDOT:PSS film thickness was measured to be 100 nm. RTA was subsequently performed in an *AnnealSys AS-One* system. This system uses incoherent halogen bulbs to heat samples at greatly enhanced rates, as monitored by the system pyrometer. The rapid thermal annealing process investigated for electrical changes involved a temperature ramp rate of 25 °C/s before a 30 s hold time at the maximum temperature in an inert Argon atmosphere. For electrical contacts, 200 nm of Al was then thermally evaporated directly onto the PEDOT:PSS film using a shadow mask technique that formed square contact pads with 500 μm sides at varying distance intervals on the slide for TLM. Electrical characterization of the conductivity of PEDOT:PSS film were obtained using both an HP 4155 semiconductor parametric analyzer and also a 4-point probe model 101 C from four dimensions.

To establish the highest temperature at which a device structure can be annealed, the lowest damage threshold of the material constituents of the structure has to be established. From prior work, it was established that the highest RTA processing temperature for PEDOT:PSS is 300 °C. Annealing at higher temperatures causes the film to demonstrate signs of damage. It was further established that of the materials utilized in this structure, ITO displayed the lowest damage threshold, which was found to exhibit signs of deterioration in its physical and electrical properties when annealed at temperatures above 200 °C. The damage threshold for ITO was determined by analyzing current stability under consecutive biasing. These results can be seen in Figure 1, which is a graph of 25 consecutive voltage sweeps from −5 to 5 V. The samples annealed at 250 °C and 300 °C show significant variation in conducted current through the ITO film and the expected linear relationship seen in the unprocessed film is destroyed as well. To properly adhere to all material constraints for these and any future devices involving ITO/PEDOT:PSS interfaces, RTA processing was subsequently limited to 200 °C. Initially, a linear TLM structure, utilizing thermally evaporated aluminum contacts was tested. The inset in Figure 2 is a schematic of the linear TLM structure used for analysis, with distances between pads ranging from 650 to 3550 μm. In Figure 2, the results of the TLM I-V measurements are displayed as a plot of the overall resistance change with respect to length following removing the effects of the contact resistance between the aluminum contacts and the PEDOT-PSS film. From these results, the reduction in slope, corresponding to a decrease in sheet resistivity of the PEDOT:PSS, with increased annealing temperature can be determined. By performing a linear fit to the data, a reduction in slope from 0.075 Ω/μm in the unannealed sample to 0.054 Ω/μm in the 200 °C annealed sample was determined. To further elucidate and verify these results, 4-point probe measurements of the PEDOT-PSS films spun on insulating glass were performed to compare the electrical properties of the as-spun and annealed films. The measurement results are given in Table I. They demonstrate the systematic reduction of sheet resistivity with increased RTA processing temperature, and a comparison between the unannealed sample and the film annealed at 200 °C shows a resistivity drop from 7.60 to 2.54 $\Omega/\square$. The reduction in the sheet resistance with annealing temperature corroborates the TLM results, which indicates that RTA increases the in-plane conductivity of spin cast PEDOT:PSS films. While RTA was limited to 200 °C to adhere to ITO constraints, previous spectroscopic results indicate that this trend persists up to annealing at 300 °C.[9]

In comparison to conventional oven annealing, this is a promising result as the anneal time is only 30 s at high temperatures as opposed to hours, preventing potentially destructive heating effects, especially at temperatures greater than 200 °C.[12] While annealing up to 300 °C was not performed due to adherence with the conductive ITO layer, spectroscopic evidence from previous studies indicate the suitability of RTA for processing at temperatures where conventional annealing may cause degradation.

PROBING THE ROOT CAUSES BEHIND THE CONDUCTIVITY ENHANCEMENT

To investigate the root causes behind this sheet conductivity increase, a variety of spectroscopic analyses were performed. Raman spectroscopy has been previously used to study doping mechanisms for electrochemically synthesized PEDOT films.[13] The Raman spectra of these films revealed a significant change in the position of $C_\alpha=C_\beta$ stretching bands with various levels of different dopants. It has also been shown that the relative intensity of the symmetric $C_\alpha=C_\beta$ stretching bands associate well with the doping level, and hence provided a valuable means for estimating the doping level of PEDOT films accurately from Raman spectra. Unlike conventional process monitoring techniques, such mass spectroscopy, UV-Vis or near-infrared (NIR) spectroscopy, and other chromatography methods, Raman spectroscopy provides high chemical selectivity, requires no additional sample preparation procedures and more importantly is non-destructive and not affected by water.

For optical characterization, high conductivity grade PEDOT:PSS aqueous dispersion from Sigma-Aldrich was spin coated onto pre-cleaned ITO substrates. The ITO was purchased from Delta Technologies Inc. and had a sheet

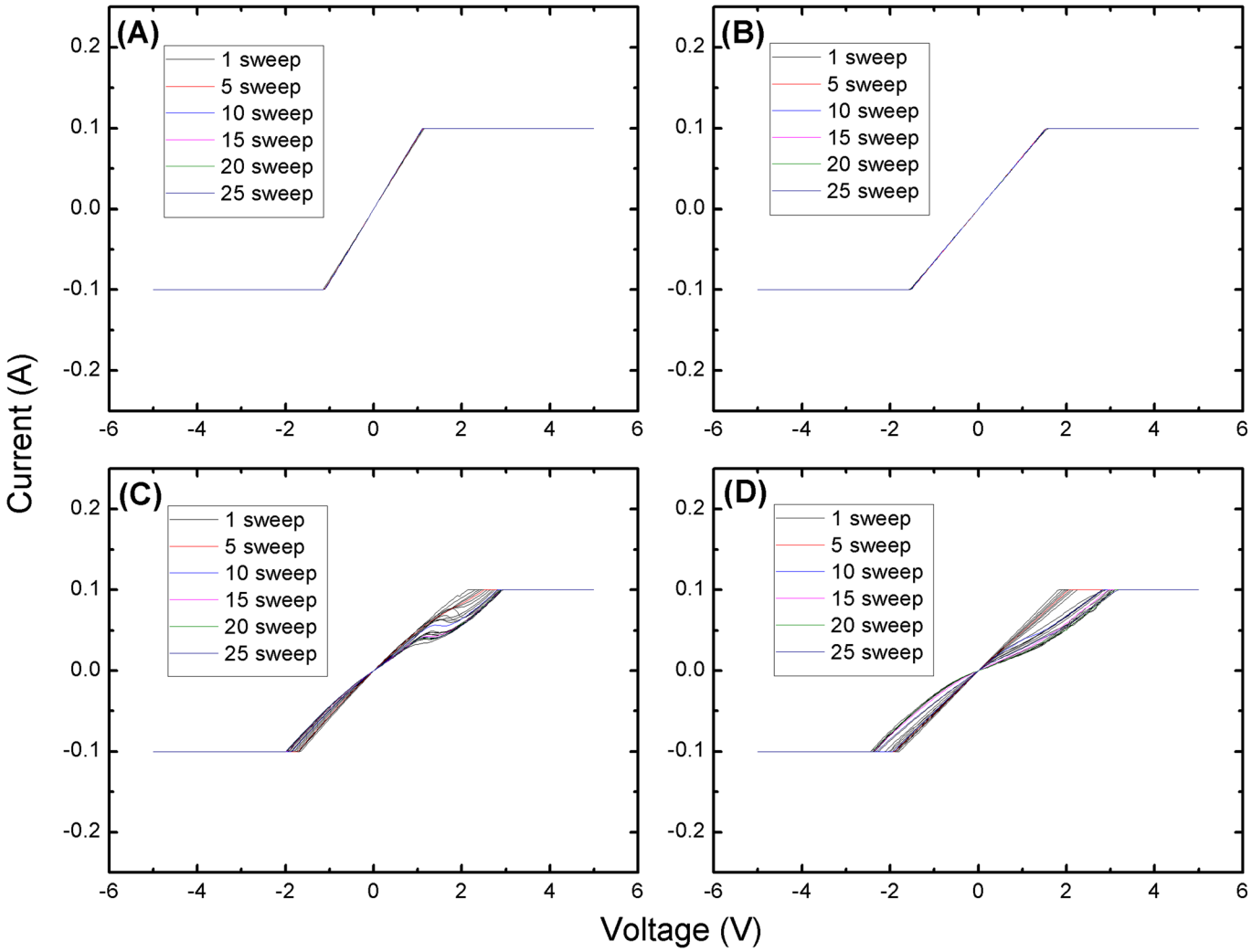

FIG. 1. IV curves for ITO layers subjected to various annealing conditions, where the ITO was subjected to rapid thermal annealing at (B) 200 °C, (C) 250 °C, (D) 300 °C as well as no annealing (A). The graphs depict the current response to 25 consecutive voltage sweeps from −5 to 5 V. At higher annealing temperatures, the variation in conduction over the 25 sweeps due to material degradation is evident.

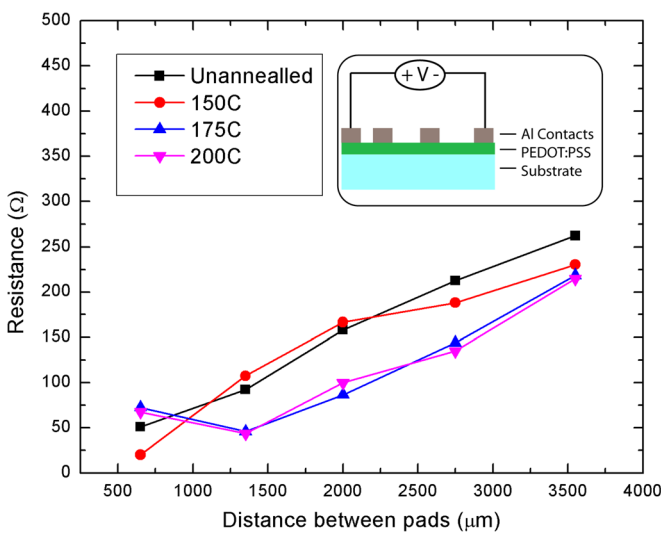

FIG. 2. A plot of the PEDOT:PSS sheet resistivity on a glass substrate obtained through I-V measurements on a linear TLM structure to remove the effects of the contact resistance. The distance between the Al contacts was varied from 650 to 3550 μm. Through a linear fit of the data, the reduction in sheet resistance with increased annealing temperature is evident. The inset is an illustration of the structure fabricated for analysis.

TABLE I. 4-pt probe measurements of the annealed PEDOT:PSS films on glass substrate.

Annealing temperature (°C)	Sheet Resistivity Ω/□
Unannealed	7.60×10^0
150	3.30×10^0
200	2.54×10^0

resistivity in the range of 4-8 Ω/□. Average polymer film thickness of 300 nm was determined by ellipsometry. RTA was again performed in an *AnnealSys AS-One* system. The samples for optical analysis were heated in an inert argon atmosphere up to temperatures ranging between 200 °C and 280 °C with intervals of 20 °C for a duration of 300 s and with a ramp time of 15 s. Raman spectroscopy was used first to study the effects of the RTA on the PEDOT:PSS films. Raman spectra were obtained using a HR 800 Horiba Jobin Yvon with a 632 nm excitation wavelength. A Gaussian/Lorentzian fitting routine was applied across the entire spectrum to quantify the peaks. Samples with annealing temperatures above 300 °C were not studied optically, as the

polymer samples were degraded such that no peak assignment with any certainty could take place.

Unannealed Raman spectrum of the spin coated PEDOT:PSS on ITO is shown in Figure 3(a). In order to achieve better accuracy when assigning the Raman modes, the Raman spectrum of PSS was obtained to serve as a reference. Due to the weak Raman scattering cross section of PSS, it was necessary to spin it on crystalline Si instead of ITO on glass in order to get an intelligible signal. The spectrum is shown in Figure 3(b). As can be seen in the spectrum, the PSS contributes very little to the Raman spectrum obtained from PEDOT:PSS. Raman mode frequencies and intensities for the PEDOT:PSS have been routinely correlated with the optical and electronic structures of poly and oligothiophenes with structures that contain π-conjugated backbone. Particularly, Raman modes in the 1100-1700 cm^{-1} range for PEDOT are not dispersive as no apparent shift of line positions were observed with the 632 nm excitation laser line.[14] As such, the following bands are mainly related to the PEDOT polymer structure and are strongly visible in the spectra: 1563 cm^{-1} and 1532 cm^{-1} are assigned to the asymmetric C_α=C_β stretching, 1421 cm^{-1} to symmetric C_α=C_β (−O) stretching, 1368 cm^{-1} to C_β-C_β stretching, 1256 cm^{-1} to C_α-C_α inter-ring stretching, 1093 cm^{-1} to C-O-C deformation, 989 cm^{-1} to oxyethylene ring deformation, 701 cm^{-1} to symmetric C-S-C deformation, 577 cm^{-1} to oxyethylene ring deformation, and 437 cm^{-1} to SO_2 bending. The peak positions and their assignment are all in good agreement with reported literature data that are consistent with the invariant relative peak positions with excitation wavelengths.[15,16]

From the Raman spectra, it was evident that annealed PEDOT-PSS films exhibited significant modification of their electronic and vibrational properties as shown in Figure 3(c), which plots the Raman spectra of the annealed and unannealed samples. Notable differences between the Raman modes of the annealed and unannealed films are evident in the region between 1100 cm^{-1} and 1700 cm^{-1}. New peak appearance, peak position shift, and changes in their shape are all observed in both the symmetric and asymmetric C_α=C_β band of the PEDOT. Curve fitting of the C_α=C_β band profiles for one of the annealed PEDOT films are shown in Figure 4(a). When monitoring the shift of these

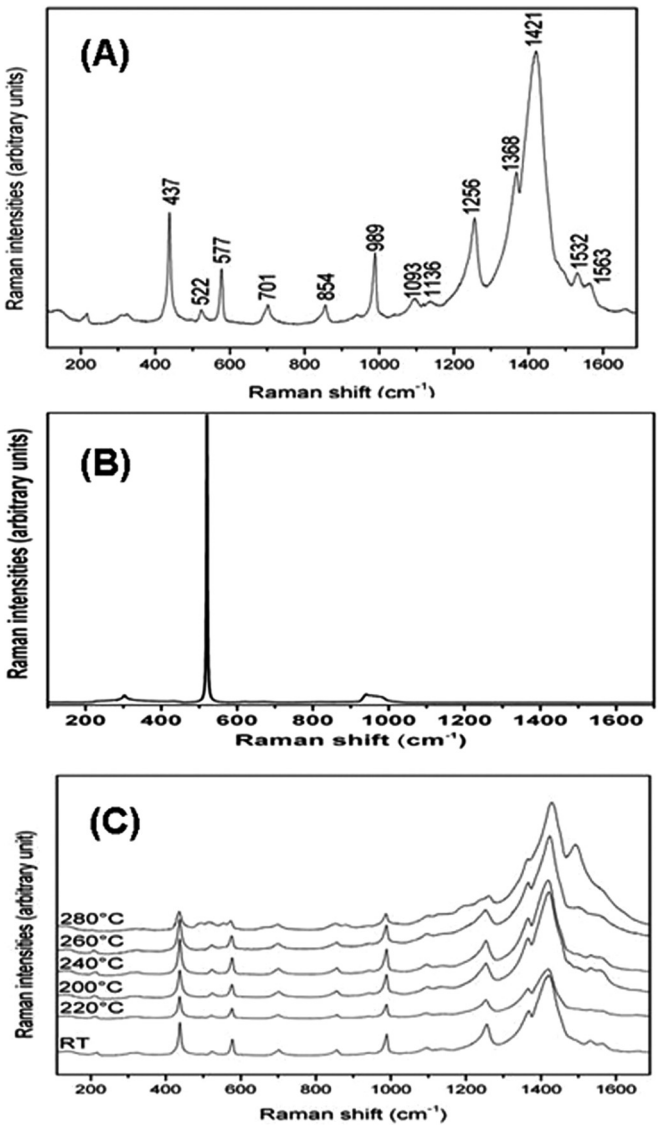

FIG. 3. (A) Raman spectra of PEDOT:PSS film as-formed film. Key modes have been identified. (B) The Raman spectrum of PSS on a Si substrate. (C) Detailed Raman spectra of PEDOT:PSS film having undergone rapid thermal annealing at different temperatures ranging from 220 °C to 280 °C.

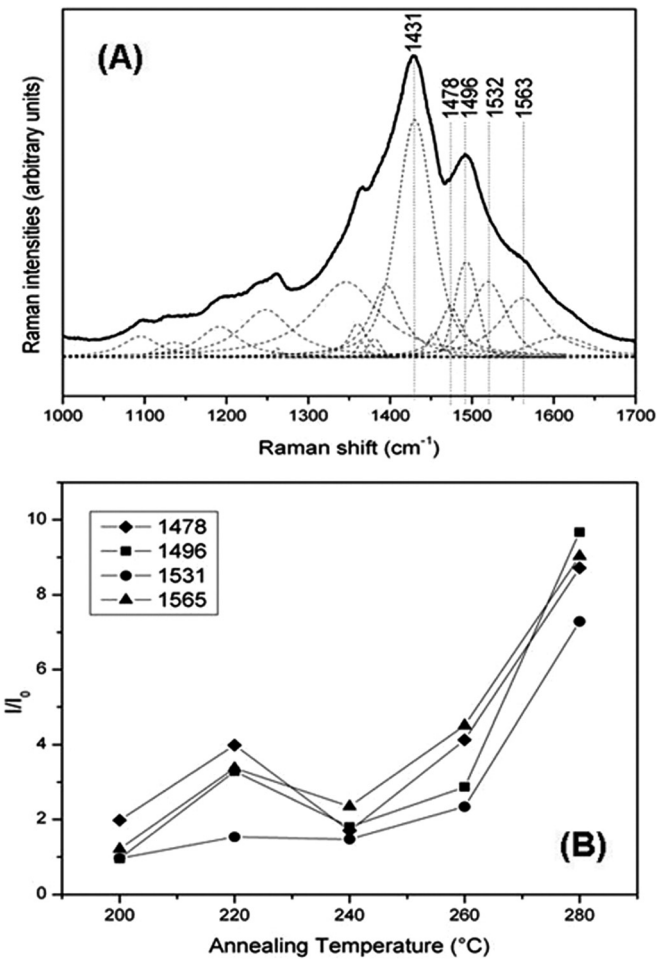

FIG. 4. (A) Curve fitting analysis of relevant $C_\alpha = C_\beta$ stretching vibrations. (B) Relative ratios of relevant integrated intensities of $C_\alpha = C_\beta$ stretching vibrations from the annealing process in the range of 1100-1700 cm^{-1} in comparison to annealing temperature. With increased temperature, a significant change in peak ratio can be observed correlating to changes in the PEDOT:PSS structure.

modes as a function of annealing, it is found that the symmetric $C_\alpha{=}C_\beta(-O)$ stretching peak at 1421 cm^{-1} for the unannealed sample shifts to a higher wavenumber and reaches 1430 cm^{-1} for the sample annealed at 280 °C. Furthermore, amongst asymmetric modes, certain peaks become more dominant upon annealing. A new peak appears at 1478 cm^{-1} while the peak at 1496 cm^{-1} increases its relative intensity until it becomes a distinct band in the sample annealed at 280 °C. Other noticeable modes also include peaks at 1531 cm^{-1} and 1563 cm^{-1} that are related to asymmetric $C_\alpha{=}C_\beta$ stretching.[15] Relative peak intensities of these peaks as shown in Figure 4(b) are indicative of the degree of PEDOT polymer chain doping, which monotonically increases with higher annealing temperature while the polymer microstructure remains intact. These changes in the band intensity ratio provide evidences that electronic structure of the PEDOT is modified with RTA and the degree of modification varies with annealing temperature.

XPS was also used to examine the surface composition profiles of PEDOT-PSS film before and after annealing. For XPS, the samples were analyzed using a Thermo Scientific Theta Probe XPS spectrometer (ThermoFisher, E. Grinstead, UK). The samples were run in standard mode (i.e., all angle collected (60° angular acceptance)) for the survey spectra and the region spectra. A monochromatic Al K_α X-ray source was used, with a spot area of 300 μm^2. Charge compensation was provided utilising the combined e^-/Ar^+ flood gun. Position of the energy scale was adjusted to place the main C 1s feature (C-C) at 285.0 eV. Peak areas were obtained from spectra run in low resolution mode (pass energy—200 eV). Elements of interest (C, S, and O) were also run in high resolution mode (30 eV pass energy). The instrument and all data processing were performed using the software (AVANTAGE) provided with the instrument. Peak areas, line shapes, and intensities of C 1s, O 1s, and S 2p high resolution core level spectra were monitored. Observed changes in relative signal ratios were analyzed to deduce, which elements are involved in the species generated. In all spectra reported here, small circles represent the data points whereas the solid lines represent fits to the data used for analysis.

The peak fitting of core level C 1s spectra is shown in Figures 5(a) and 5(b) for the unannealed and the annealed film at 280 °C, respectively. The spectrum for the unannealed film displays three components with binding energies at 284.9 eV, 285.8 eV, and 286.7 eV. This correspond to C-H/C-C (curve 1), C-C-O (curve 2), and C-S (curve 3) of the PEDOT:PSS, respectively. In comparison to the C1s spectra obtained for the unannealed films, the film annealed at 280 °C develop some significant changes in the C 1s spectra, where the high-binding energy side of the main peak representing the C-S and C-C-O exhibit reduction in intensity compared to the original peaks.

This is indicative that the composition of the outermost surface of the film becomes rich in alkyl carbons due to the electronic charge gained by some of these carbon sites. More importantly, any sign of polymer photo thermal degradation, such as oxygen inter-diffusion into the polymer microstructure was not observed by the XPS analysis in any of the films.[17] This suggests that the quality of the films was

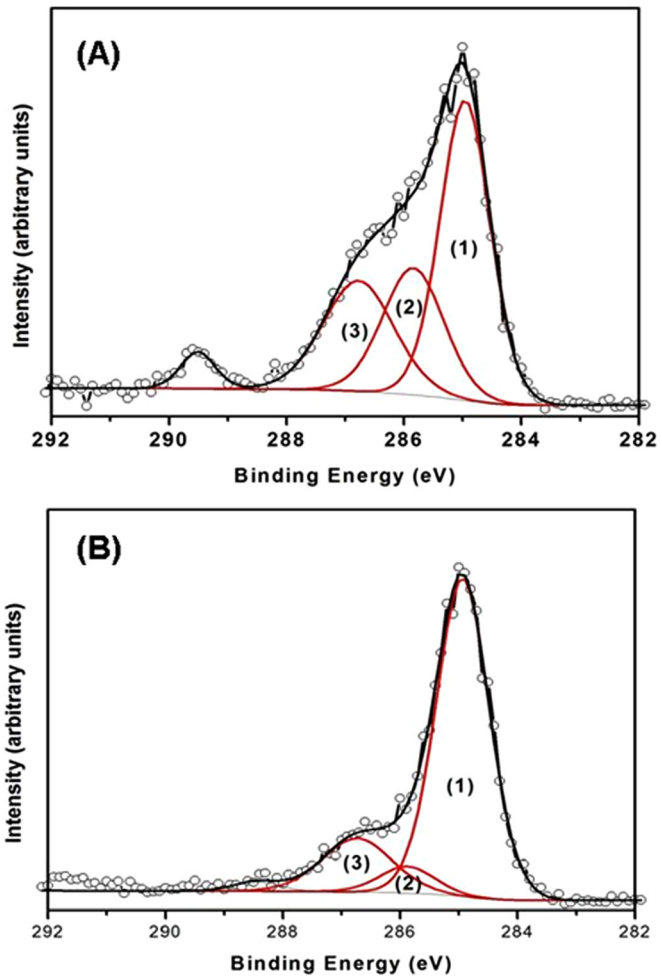

FIG. 5. Deconvolution of C 1s core level from the XPS analysis of PEDOT:PSS film on ITO (A) as-formed film. (B) 280 °C thermally annealed film.

maintained upon annealing at the temperatures used, in contrast to the degradation induced by conventional oven annealing at these temperatures.

The S 2p core level spectra, as shown in Figures 6(a) and 6(b), for the unannealed sample and the sample annealed at 280 °C show, as expected, two signature peaks. Each peak involves contributions from a spin-split doublet, S $2p_{3/2}$ and S $2p_{1/2}$, with 1.2 eV energy splitting and 1:2 intensity ratio.[18,19] The S 2p contribution peaks at 163.7 eV (curve 1) and 164.9 eV (curve 2) corresponds to sulfur atoms of the PEDOT and those at higher binding energies at 167.7 eV (curve 3) and 168.9 eV (curve 4) belong to PSS because of the electronegative oxygen attached to sulfur atom in the sulfonate fragment of the PSS.[17]

As can be seen in Figure 6, the intensity of S 2p contribution from the PEDOT moiety significantly increases and that of PSS decreases with increasing the annealing temperature. This increase can be attributed the enhancement of the contribution of the PEDOT component to the signal. This in turn suggests the formation of a film with a PEDOT-accessible surface as the annealing temperature is increased. Such a finding is remarkable as it is contrary to what is expected for PEDOT:PSS interfaces without anealing.[20] This can have implications on the control of the quality of

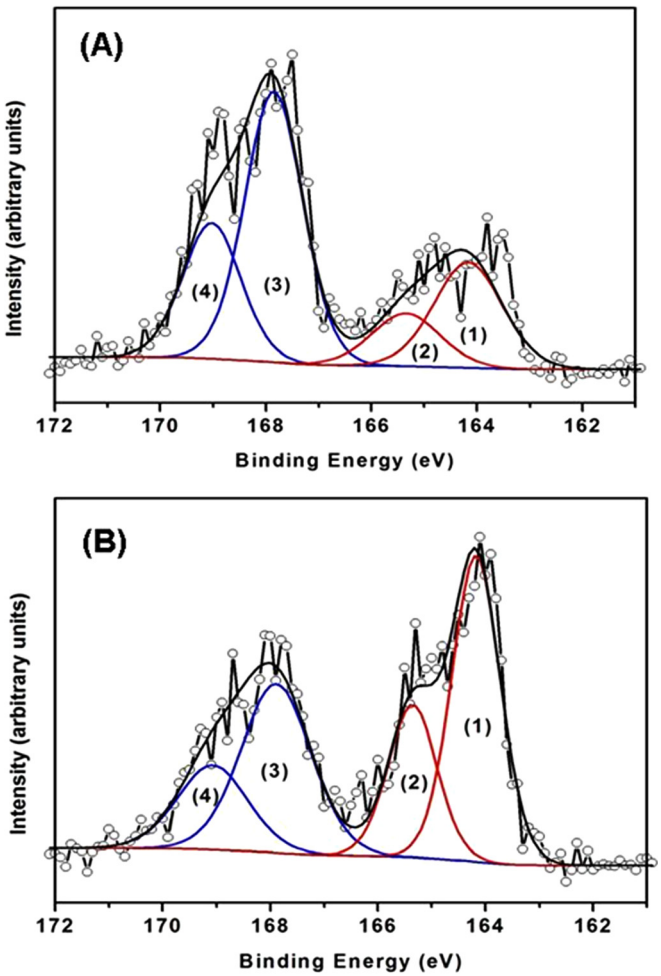

FIG. 6. Deconvolution of S 2p core level from the XPS analysis of PEDOT:PSS film on ITO (A) as-formed film. (B) 280 °C thermally annealed film.

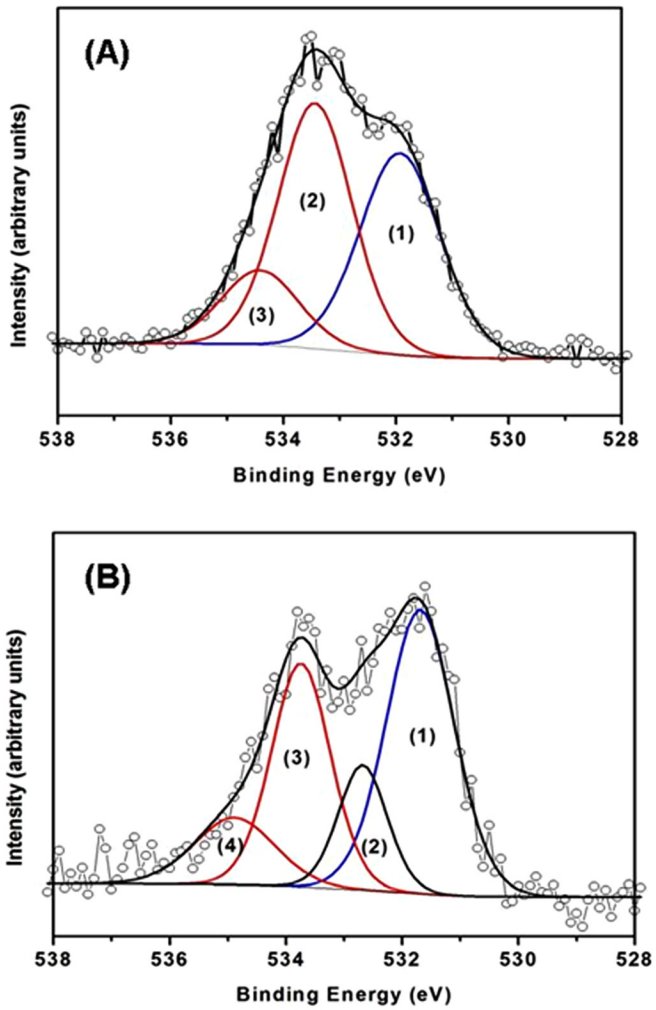

FIG. 7. Deconvolution of O 1s core level from the XPS analysis of PEDOT:PSS film on ITO (A) as-formed film. (B) 280 °C thermally annealed film.

electrical contacts that can be formed on such films. Despite of some intensity reduction in the S 2p peaks with annealing neither does the line shape of the S 2p contribution from the PSS changes form nor does the peak position shift to a lower binding energy. Equally significant, signs of detachment of sulfonate group from the PSS polymer chain were not observed in the XPS analysis.[16] This is all indicative of the intact quality of the films upon annealing at the temperatures used, which is unique to this annealing technique in comparison to conventional oven annealing.

XPS high resolution spectra for the O 1s deconvolved peaks for unannealed sample are shown in Figures 7(a) and 7(b). The spectra reveal three major components at 531.8 eV (curve 1), 533.1 eV (curve 2), and 534.4 eV (curve 3). In both the unannealed and 200 °C annealed films, the strongest intensities of O 1 s peaks are centered at 533.1 eV (curve 2) assigned to the (C-O-C) of the PEDOT and 531.8 eV (curve 1) corresponding to (O=S) in the PSS.[21] For the 280 °C annealed sample as in Figure 7(b), the peaks at 534.9 eV (curve 4) and at 531.7 eV (curve 1) remain almost invariant. A new peak emerges at 532.6 eV (curve 2) while the peak at 533.7 eV (curve 3) corresponding to C-O-C bond of the PEDOT increased in intensity. This suggests a modification of electron charge distribution along the C-O-C bond of the PEDOT as a result of the annealing process, which sheds light on the mechanisms responsible for the changes in conduction properties observed from electrical measurements.

The interface between the PEDOT:PSS and ITO is also crucial in determining the electrical properties for future device application of these materials. To better understand the nature of ITO/polymer interface and the morphological changes that may occur in the PEDOT:PSS films as a result of thermal annealing, AFM images of PEDOT:PSS layer were taken before and after annealing at different temperatures. A Nanoscope IIIa AFM (Digital Instrument) was used to analyze the topography and the roughness of the films before and after the annealing process. Images were acquired in tapping mode. The measurements were performed in air at 27 °C, using a Si cantilever with a spring constant of ca. 20-100 N/m, a tip radius of 5–10 nm, and resonance frequency of about 300 KHz. As shown in Figure 8(a), unannealed PEDOT:PSS films display smooth bundles of grain-like structures that are attributed to molecularly phase separated PEDOT:PSS chains[19] and with rms roughness of 7.20 nm. Films annealed at 200 °C and 280 °C, the rms roughness become 11.50 nm and 7.50 nm, respectively. The surface roughness increases as the annealing temperature is increased

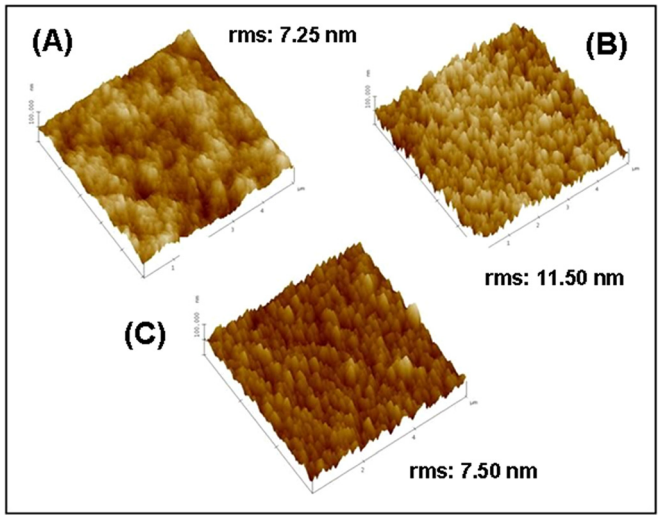

FIG. 8. AFM tapping mode height images of PEDOT:PSS film on ITO (A) as-formed film. (B) 200 °C annealed and (C) 200 °C thermally annealed film.

from room temperature to 200 °C, but further annealing temperature increase to 280 °C, the surface becomes less rough compared to the films annealed at 200 °C. This roughness can be ascribed to the repulsion forces arising from enhanced conductivity of the films.

It is important to note that the PEDOT:PSS films annealed at 200 °C exhibit a coarse morphology and broad hill-like structures sticking vertically out from the planar ITO substrate as can be seen in Figure 8(b). These hill-like structures are indicative of the formation of PEDOT-rich domains, which are composed of time stable, molecularly doped PEDOT structures that are more readily accessible than those unannealed and annealed at 280 °C. Moreover, the resulting spatial separations of the PEDOT-rich domains could diminish their electrostatic interaction with PSS chains.

CONCLUSION

In conclusion, through the application of RTA to thin film PEDOT:PSS films, the sheet conductivity has been increased by nearly a factor of three, demonstrating the importance and potential of RTA for post deposition processing to improve the characteristics of organic thin films and devices. The conductivity increase was measured through both TLM measurements and also 4-pt probing. Upon spectroscopic investigation by Raman spectroscopy, XPS, and AFM, this conductivity enhancement has been attributed to microstructural variations and morphology of PEDOT:PSS films. This study has clearly shown that annealing of PEDOT:PSS films induces distinctive structural modifications of the PEDOT domains, which upon annealing emerge onto the film interface. This can have a significant impact on the contacts that can be achieved between this material system and metals amongst other materials. It also strongly suggests the formation of stable doped PEDOT structures with high optical density of collective C=C/C-C stretching vibrations that can be easily interrogated by non destructive Raman spectroscopy. Critical to any device application of these films is also their chemical and thermal stability after brief exposure to the RTA condition. XPS analysis of these films clearly confirmed their chemical and molecular integrity, while AFM exposed outermost characteristics of PEDOT surface morphology. Furthermore, these observations lead us to gain further insight as to the potential for device performance improvement through the RTA process.

ACKNOWLEDGMENTS

We thank the Surface Interface Ontario at the Chemical Engineering and Applied Chemistry at the University of Toronto Facility for XPS analysis.

[1]C. K. Chiang, C. R. Fincher, Y. W. Park, A. J. Heegar, H. Shirakawa, E. J. Louis, S. C. Gau, and A. G. MacDiarmid, Phys. Rev. Lett. **39**, 1098 (1977); H. Shirakawa, E. J. Louis, A. G. MacDiarmid, C. K. Chiang, and A. J. J. Heegar, J. Chem. Soc. Chem. Commun. **16**, 578 (1977).
[2]M. Jaiswal and R. Menon, Polym. Int. **55**, 1371 (2006); S. Athanasopoulos, J. Kirkpatrick, D. Martinez, J. M. Frost, C. M. Foden, A. B. Walker, and J. Nelson, Nano Lett. **7**, 1785 (2007).
[3]J. L. Reddinger and J. R. Reynolds, Adv. Polym. Sci. **145**, 57 (1999); A. Facchetti, M.-H. Yoon, C. L. Stern, H. E. Katz, and T. J. Marks, Angew. Chem. Int. Ed. **42**, 3900 (2003); H. Nakashima, K. Furukawa, K. Ajito, Y. Kashimura, and K. Torimitsu, Langmuir **21**, 511 (2005).
[4]S. Allard, M. Forster, B. Souharce, H. Thiem, and U. Scherf, Angew. Chem. Int. Ed. **47**, 4070 (2008); F. J. M. Hoeben, P. Jonkheijm, E. W. Meijer, and A. P. H. Schenning, Chem. Rev. **105**, 1491 (2005).
[5]L. B. Groenendaal, F. Jonas, D. Freitag, H. Pielartzik, and J. R. Reynolds, Adv. Mater. **12**, 481 (2000); S. Kirchmeyer and K. J. Reuter, Mater. Chem. **15**, 2077 (2005); R. H. Friend, R. W. Gymer, A. B. Holmes, J. H. Burroughes, R. N. Marks, C. Taliani, D. D. C. Bradley, D. A. Dos Santos, J. L. Bredas, M. Logdlund, and W. R. Salaneck, Nature **397**, 121 (1999).
[6]H. Sirringhaus, N. Tessler, and R. H. Friend, Science **280**, 1741 (1998); Y. Xu, J. Peng, Y. Mo, Q. Hou, Y. Cao, Appl. Phys. Lett. **86**, 163502 (2005); J. Jang, M. Chang, and H. Yoon, Adv. Mater. **17**, 1616 (2005); J. Joo, S.-K. Park, D.-S. Seo, S.-S. Lee, H.-S. Kim, K.-S. Ryu, T.-J. Lee, S.-H. Seo, and C.-J. Lee, Adv. Funct. Mater. **15**, 1465 (2005); D. M. Delongchamp, M. Kastantin, and P. T. Hammond, Chem. Mater. **15**, 1575 (2003); C.-C. Chang, L.-J. Her, and J.-L. Hong, Electrochim. Acta **50**, 4461 (2005).
[7]A. Elschner, S. Kirchmeyer, W. Lövenich, U. Merker, and K. Reuter, *PEDOT: Principles and Applications of an Intrinsically Conductive Polymer* (CRC, Boca Raton, 2011), p. 147.
[8]S. A. Rutledge, A. A. Farah, J. Dinglasan, D. J. Anderson, A. Das, J. Goh, C. Goh, and A. S. Helmy, J. Phys. Chem. C **113**, 20208 (2009).
[9]A. Schaarschmidt, A. A. Farah, and A. S. Helmy, J. Phys. Chem. B **113**, 9352 (2009).
[10]F. Roozeboom, *Advances in Rapid Thermal Annealing and Integrated Processing*, Nato ASI Series, Series E: Applied Science Vol. 318 (Kluwer Academic, 1996); V. E. Borisenko and P. J. Hesketh, *Rapid Thermal Processing of Semiconductors* (Plenum, New York, 1996); H. Fukuda, *Rapid Thermal Processing for Future Semiconductors: Proceedings of RTP 2001* (Elsevier, Ise-Shima Japan, 2003); R. J. Singh, Appl. Phys. **63**, R59 (1998).
[11]A. J. Dhanabalan, J. K. L. van Duren, P. A. van Hall, J. L. J. van Dongen, and R. A. J. Janssen. Adv. Funct. Mater. **11**, 255 (2001); C. J. Brabec, C. Winder, N. S. Sariciftci, J. C. Hummelen, A. J. Dhanabalan, P. A. van Hall, and R. A. J. Janssen. Adv. Funct. Mater. **12**, 709 (2002); Y. Yang, Q. Huang, A. W. Metz, J. Ni, S. Jin, T. J. Marks, M. E. Madsen, A. DiVenere, and S.-T. Ho, Adv. Mater. **16**, 321 (2004); T. Kondo, S. M. Lee, M. Malicki, B. Domercq, S. R. Marder, and B. Kippelen, Adv. Funct. Mater. **18**, 1112 (2008); J. A. Bardecker, H. Ma, T. Kim, F. Huang, M. S. Liu, Y.-J. Cheng, G. Ting, and A. K.-Y. Jen, Adv. Funct. Mater. **18**, 3964 (2008).
[12]H. Huang, P. F. Miller, J. S. Wilson, A. J. de Mello, J. C. de Mello, and D. D. C. Bradley, Adv. Funct. Mater. **15**, 290 (2005).
[13]W. W. Chiu, J. Travis-Sejdic, R. P. Cooney, and G. A. J. Bowmaker, J. Raman Spectrosc. **37**, 1354 (2006); W. W. Chiu, J. Travis-Sejdic, R. P. Cooney, and G. A. Bowmaker, Synth. Met. **155**, 80 (2005).

[14]E. M. Girotto, W. A. Gazotti, and M.-A. DePaoli, J. Phys. Chem. B **104**, 6124 (2000).
[15]S. Garreau, G. Louarn, J. P. Buisson, G. Froyer, and S. Lefrant, Macromolecules **32**, 6807 (1999).
[16]S. Garreau, J. L. Duvail, and G. Louarn, Synth. Met. **125**, 325 (2001).
[17]X. Crispin, S. Marciniak, W. Osikowicz, G. Zotti, A. W. D. Van Der Gon, F. C. Louwet, M. Fahlman, L. Groenendaal, F. De Schryver, and W. R. Salaneck, J. Polym. Sci. Part B: Polym. Phys. **41**, 2561 (2003); S. Holdcroft, Macromolecules **24**, 2119 (1991); S. Holdcroft, Macromolecules **24**, 4834 (1991); M. S. A. Abdou and S. Holdcroft, Macromolecules **26**, 2954 (1993).
[18]D. G. Castner, K. Hinds, and D. W. Grainger, Langmuir **12**, 5083 (1996).
[19]J. H. Scofield, J. Electron Spectrosc. Relat. Phenom. **8**, 129 (1976).
[20]G. Grecynski, T. Kugler, and W. R. Salaneck, Thin Film Solids **354**, 129 (1999).
[21]D. Briggs and G. Beamson, Anal. Chem. **65**, 1517 (1993).